

High Fidelity Electrical Model with Thermal Dependence for Characterization and Simulation of High Power Lithium Battery Cells

Tarun Huria, Massimo Ceraolo
Department of Energy and Systems Engineering
University of Pisa
Largo Lazzarino, Pisa 56122 Italy
m.ceraolo@ing.unipi.it

Javier Gazzarri, Robyn Jackey
MathWorks
39555 Orchard Hill Place, Suite 280
Novi, MI 48375 USA
robyn.jackey@mathworks.com

Abstract— The growing need for accurate simulation of advanced lithium cells for powertrain electrification demands fast and accurate modeling schemes. Additionally, battery models must account for thermal effects because of the paramount importance of temperature in kinetic and transport phenomena of electrochemical systems. This paper presents an effective method for developing a multi-temperature lithium cell simulation model with thermal dependence. An equivalent circuit model with one voltage source, one series resistor, and a single RC block was able to account for the discharge dynamics observed in the experiment. A parameter estimation numerical scheme using pulse current discharge tests on high power lithium (LiNi-CoMnO₂ cathode and graphite-based anode) cells under different operating conditions revealed dependences of the equivalent circuit elements on state of charge, average current, and temperature. The process is useful for creating a high fidelity model capable of predicting electrical current/voltage performance and estimating run-time state of charge. The model was validated for a lithium cell with an independent drive cycle showing voltage accuracy within 2%. The model was also used to simulate thermal buildup for a constant current discharge scenario.

Keywords- high-power lithium cell; thermal model, electrical equivalent lithium cell model, state of charge, pulse discharge test, energy storage; electric vehicle, hybrid electric vehicle

I. NOMENCLATURE

BMS	battery management system
C_n	capacitor n , where n is a natural number
C_Q	cell capacity (Ah)
C_T	heat capacitance ($J m^{-3} K^{-1}$)
E_m	electromotive force of main branch
E_p	electromotive force of parasitic branch
ECM	equivalent circuit model
EKF	extended Kalman filter
I_m	current in main branch (A)
I_n	current in branch n , where n is a natural number (A)
I_p	current in parasitic branch (A)
NMC	nickel-manganese-cobalt

OCV	open circuit voltage (V)
P_s	power dissipated inside the cell (W)
Q_e	extracted charge from cell (Ah)
R_n	resistor n , where n is a natural number (Ω)
R_T	convection resistance ($W^{-1} m^{-2} K^{-1}$)
s	Laplace transform variable
SOC	state of charge
T	inner cell temperature ($^{\circ}C$)
T_a	ambient temperature ($^{\circ}C$)
V	voltage (V)
Z_p	impedance of parasitic branch (Ω)

II. INTRODUCTION

An accurate forecast of the remaining driving range of an electric vehicle (EV) is crucial to avoid range anxiety. Drivers need to know how much further they would travel before their vehicle batteries require a recharge. In addition, the battery management system should predict when batteries need replacement. The remaining charge calculation must be precise to utilize the battery's full capability. The state of charge (SOC) of a battery or pack of batteries is analogous to a fuel gauge of a conventional vehicle.

Accurate run-time SOC estimation techniques are also needed by the battery management system (BMS) for cell balancing of battery packs in vehicles with electrified powertrains. The SOC estimation must be accurate under all vehicle operating conditions, and account for changes in temperature, different rates of current, and cell aging. High temperatures, broad SOC operation ranges, and strenuous load profiles accelerate cell aging. Coulomb counting (i.e. integration of the current) is a simple technique for estimating the SOC by integrating the measured current with time. However, coulomb counting has several drawbacks. Coulomb counting depends on the current flowing from the cell into external circuits and does not account for self-discharge currents or parasitic reactions in the cell. Current measurement errors accumulate with time, and should be corrected by periodic recalibration. The maximum charge capacity of the cell depends on a number of factors, such as average

discharge current, discharge time, inner cell temperature, storage time (self-discharge), and cycle-age [1].

Equivalent circuit modeling (ECM) is the most common approach for battery numerical analysis. For lithium cells, a one or two RC block model with no parasitic branch is a common choice [1-3]. It has the advantage of being computationally simple and is easily combined with other methods such as coulomb counting with an OCV / SOC correlation for periodic recalibration during rest. The model also lends itself to the use of adaptive methods, such as extended Kalman filter (EKF) [3-5].

This paper presents a new and intuitive method for developing a non-isothermal lithium cell model. Reducing the general ECM with n RC blocks to an ECM with just a single RC block was sufficient to account for all dynamic characteristics of the cell, including nonlinear open-circuit voltage, average discharge current and inner cell temperature. A numerical parameter estimation scheme using pulse current discharge tests on high power lithium nickel-manganese-cobalt oxide (NMC) cells under different operating conditions was implemented using MATLAB[®], Simulink[®] and Simscape[™]. The parameter estimation procedure revealed dependencies of the equivalent circuit elements on SOC and temperature, which were subsequently implemented as lookup tables that defined the values of the equivalent circuit elements. The model was validated using independent experimental data, and then used for general simulation purposes. This process can be used for runtime SOC estimation.

The paper is organized as follows: Section III describes the background and model formulation, while Section IV deals with the experimental setup. The results of the experimental tests on the cells are compared with the modeling results in Section V. Section VI summarizes the work and states suggestions for future work.

III. BACKGROUND AND MODEL FORMULATION

A number of models have been developed in the past to characterize and simulate lithium cells. Detailed electrochemical models that simulate the internal dynamics of the lithium cells [6-9] are computationally-intensive, time-consuming, inflexible and unsuitable for system-level modeling or run-time applications. An alternative approach is to use equivalent circuit models (ECM) [1-3]. In this case, the goal is to establish a direct correlation between electrochemical phenomena inside the cell and the circuit elements. Their level of complexity is decided as a trade-off between the fidelity and computational effort. These models can capture nonlinear electrochemical phenomena, and yet avoid lengthy electrochemical process calculations. They are especially suitable for system-level modeling (e.g. powertrain electrification).

Most models in the current literature do not account for thermal effects. This work overcomes this limitation by including temperature as an independent variable in the look-up tables that define the circuit elements.

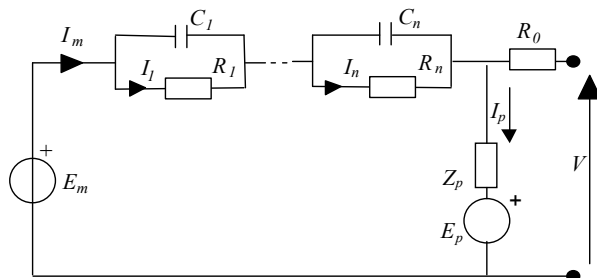


Figure 1. A general equivalent circuit model [1, 10-11] of an electrochemical cell. The number of equivalent circuit elements results in a trade-off between fidelity and complexity. The parasitic branch can be neglected for cells with high coulombic efficiencies.

Fig.1 shows the generalized ECM presented in [10-11] for lead-acid batteries, but which can be used to depict an electrochemical cell of any chemistry.

The choice of the model structure responds to a trade-off between the ability to fit experimental data and equivalent circuit complexity (and computational resources). An extremely complex equivalent circuit would fit experimental data sets well, but would be computationally expensive, making it unsuitable for embedded control applications. In general, the level of complexity should be limited by the computational resources available and the possibility of correlating each circuit component with an electrochemical phenomenon inside the cell. A model of adequate fidelity is useful for diagnosis purposes, since variation of its elements can be linked directly to a physical or electrochemical process, such as charge, capacity, or health.

Depending on the characteristics of the problem to be analyzed, the number of RC blocks typically ranges from one to two, since larger numbers increase computational effort without significantly improving model accuracy.

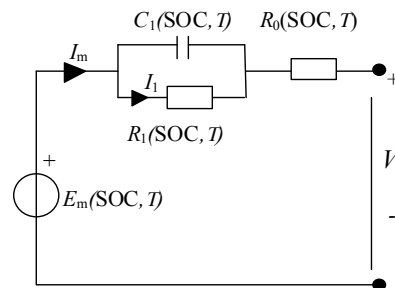


Figure 2: The model used for the paper, with $n=1$.

A single RC block model (Figure 2) is adequate for many problems of industrial relevance, and has been adopted in this work. The estimation techniques present-

ed in this paper are, however, general, and could also be applied to other equivalent circuit model topologies. The choice of the ECM of Figure 2 implied that the fitting procedure involved the estimation of four independent parameters, namely E_m , R_0 , R_1 , and C_1 , which vary with temperature and SOC of the cell.

A. Thermal modeling

The value of the ECM components depends on SOC and inner cell temperature. The inner cell temperature is assumed to be uniform, and taken as the average temperature inside the cell. This cell temperature can be computed by solving the heat equation of a homogeneous body exchanging heat with the environment:

$$C_T \frac{dT}{dt} = -\frac{T-T_a}{R_T} + P_S \quad (1)$$

Applying a Laplace transformation:

$$T(s) = \frac{P_S R_T + T_a}{1 + R_T C_T s}$$

where the meaning of the variables are reported in Section I.

Practical applications require a combination of cells rather than a cell in isolation. In general, the thermal parameters of cell packs are different from those of isolated cells, although this case is not considered here, but will be the subject of a future contribution.

B. Cell capacity and state of charge

The cell capacity (extractable charge) depends upon a number of factors, including:

- average cell discharge current and discharge time
- inner cell temperature
- value of the end-of-discharge voltage
- storage time (self-discharge)
- number of charge-discharge cycles that the cell has undergone (aging)

For short periods of time we can restrict the list above to average cell discharge current, discharge time, and inner cell temperature.

$$\text{Hence, cell capacity, } C_Q = C_Q(I, T) \quad (2)$$

Assuming the cell to be fully charged at time $t=0$, the *extracted charge*, Q_e is defined as:

$$Q_e(t) = \int_0^t I_m(\tau) d\tau \quad (3)$$

Then, the state-of-charge (SOC) is:

$$\text{SOC} = 1 - Q_e / C_Q \quad (4)$$

where C_Q is the capacity of the cell at the temperature and discharge current considered. Consequently, any SOC definition should consider the conditions under

which a cell is discharged and refer to the particular discharge current and temperature under which the SOC has been evaluated.

C. Runtime determination of state of charge

The most common technique for determining the SOC during runtime is to integrate the current output from the cell over time (coulomb counting). Since this simple technique does not account for current measurement errors or parasitic phenomena (especially at end-of-charge), periodic error compensation is needed. The most effective technique for error elimination is an SOC-OCV (open circuit voltage) correlation curve [13].

D. Equivalent circuit model parameters

Each element of the equivalent circuit of Figure 2 is a function of SOC and temperature. Specifically:

$$R_0 = R_0(\text{SOC}, T) \quad (5.1)$$

$$R_1 = R_1(\text{SOC}, T) \quad (5.2)$$

$$C_1 = C_1(\text{SOC}, T) \quad (5.3)$$

$$E_m = E_m(\text{SOC}, T) \quad (5.4)$$

The parameter estimation routine was run for a range of discharge experiments at different temperatures. The results provide two-dimensional look-up tables each of these four equivalent circuit elements.

IV. EXPERIMENTAL SETUP

A. Cell test setup

Power-oriented 31Ah lithium ion cells of the $\text{LiNi}_x\text{Mn}_y\text{Co}_z\text{O}_2$ (NMC) chemistry [13] were tested to verify the model efficacy at three different temperatures of 5°C, 20°C and 40°C. The experimental setup consisted of:

1) Charging System

The charging system was driven by an Ametek® Sorensen® 60kW programmable DC power supply (Model SPS60X250-K02D). The device allowed charging the equipment under test with a completely programmable input voltage and current profile and was fully remote controlled via the General Purpose Interface Bus (GPIB) standard interface.

2) Discharging System

The discharging system was driven by a 6kW-500A Zentro-Elektrik™ Electronic Load (Model EL 6000). The device allowed discharging the cell under test in constant current mode, constant voltage mode, constant power mode, or constant conductance mode, and was fully remote controlled via the GPIB standard interface.

3) Measurement System

A digital multi-meter measured the voltage while the current was measured using a shunt (for high currents) and a Hall-sensor current transducer (for low currents)

respectively. The cell voltage could be measured and controlled through a 16-bit multifunctional National Instruments® data acquisition board. Ambient and device temperatures were measured and controlled using two RTD (PT100) transducers connected to two multi-meters.

B. Test Cycle Control

The test cycle was implemented to control the charging, discharging, and measurement systems using GPIB standard interface and digital I/O of a data acquisition card.

C. Description of characterization tests

Pulse discharge characterization tests were conducted on the 31Ah cells at three different temperatures. The cell was initially charged and then subjected to partial discharge-rest phase cycles. At the end of each one-hour rest the voltage was found to be stable enough so as to be considered a good estimate of the OCV. The experiment determined the response of the cell to the current pulses, providing a mechanism to evaluate the parameters for the cell model. The SOC was derived based on coulomb counting of the current drawn from the cell at each step.

V. MODELING AND SIMULATION

The numerical analysis proposed here consisted of a parameter estimation / validation stage, and a simulation stage. During parameter estimation, a discharge profile was iteratively simulated and its results compared with experimental data. The ECM was created using Simscape™ blocks and Simscape™ language. The drawing shown in Figure 4 represented the circuit diagram with a single RC block. Each of the circuit elements was a subsystem consisting of custom electrical blocks, and blocks to calculate the properties of the circuit element.

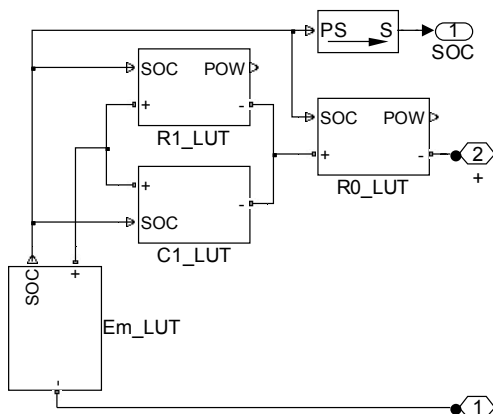


Figure 3. Simscape™ Equivalent Circuit Model

The resistive circuit elements were modeled as variable resistors, as shown in Figure 4. These were modeled based on Ohm's Law, though a minimum re-

sistance value was used to prevent the differential equation solver from entering a bad state during parameter estimation or simulation. The real power of the resistive elements was also calculated for later use in simulation of thermal dynamics. The value of the resistance was provided by a lookup table with one or two inputs of SOC and temperature.

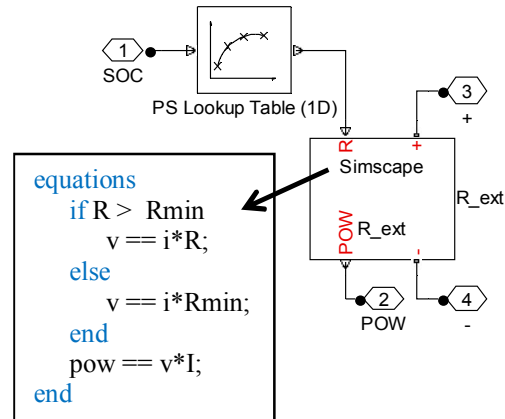


Figure 4. Resistive Circuit Element and Simscape™ Language Code

The performance of lithium cells varies significantly from cell to cell. The empirical equation approach typically used for lead-acid batteries as in [15] could not be used for lithium chemistry. Lookup tables were chosen for parameterization of the circuit elements for two reasons. One is that lookup tables are very flexible. Second, the pulse discharge technique provides sufficient cell performance information about the open-circuit voltage and RC network at each pulse for a numerical optimizer to isolate each parameter and each breakpoint within the lookup tables.

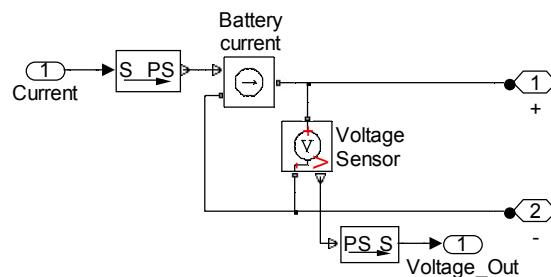


Figure 5. Simscape™ Charging Circuit

For parameter estimation, each temperature was considered independently. The lookup tables for each circuit element were chosen to be based on 7 different points of SOC, with SOC breakpoints spaced with a bias slightly toward low and high SOC. More points could have been used, but more breakpoints would have provided a diminishing benefit for two reasons. One was that more parameter values would slow down the parameter esti-

mation. The second was that the discharge pulses of 10% SOC would only provide the parameter estimator with good data near 10% SOC increments. Excessive breakpoints may have led to having too many parameters that were not well exercised in the data, which is a known problem when optimizing unconstrained lookup tables [15].

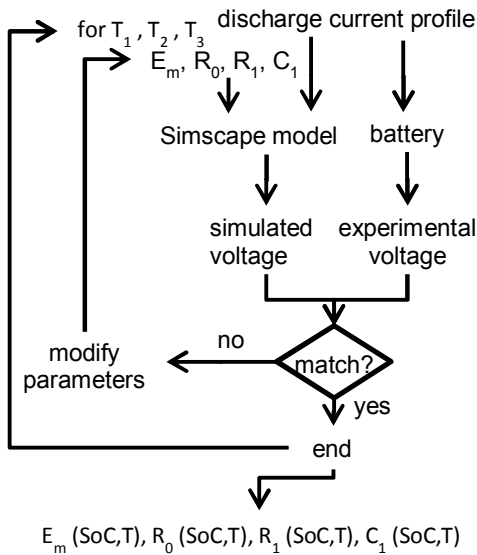


Figure 6. Flow diagram of the parameter estimation procedure

The parameters were determined using the parameter estimation tool in Simulink Design Optimization™. To enable the estimation, the Simscape™ ECM was connected to a simple charging circuit model using an ideal current source and a voltage sensor, as shown in Figure 5. The estimation was automated using the command line parameter estimation capability.

The pulse discharge curve for each temperature was run individually through an estimation task. This produced a set of one-dimensional lookup tables versus SOC for the four parameters at each temperature. To produce these lookup tables, Simulink Design Optimization™ iteratively simulated the discharge profile in Simscape™ while comparing the simulation results with experimental data. The nonlinear least-squares algorithm was used. This algorithm computed the error gradient across each of the 28 parameters (4 tables * 7 breakpoints) to minimize the sum of squared error. The flow diagram of Figure 6 illustrates the parameter estimation steps.

Repeating this process at three different temperatures (5°C, 20°C, and 40°C) resulted in four sets of data that characterized the cell chemistry under consideration: $E_m(SoC,T)$, $R_0(SoC,T)$, $R_1(SoC,T)$, and $C_1(SoC,T)$. These values, in addition to a linear interpolation process, constituted the two-dimensional look-up tables that determined the values of the

equivalent circuit elements during the simulation stage. The resulting model assumed that cell impedance did not change significantly due to the magnitude of the discharge current. The dependence on current magnitude may be investigated more closely in a future work.

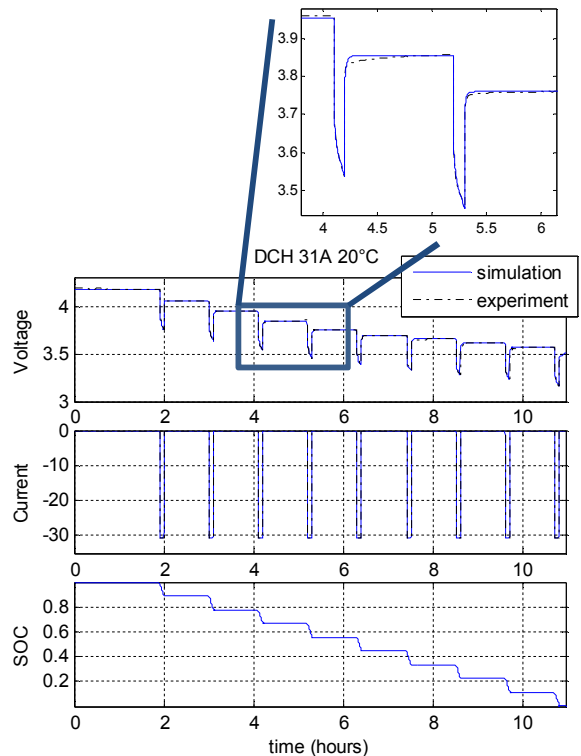


Figure 7. Experimental (- -) and simulated (-) discharge curves for a 31Ah cell at 20°C at the end of the estimation process. The cell under test shows first-order dynamics, which is effectively captured by the equivalent circuit simulation. The cell potential (top) drops with decreasing SOC (bottom), as the cell is discharged with a set of 31A pulses (middle).

Figure 7 shows the agreement between experimental and final simulated voltage, current, and SOC, at 20°C. The simulation reproduced the nine discharge pulses and was able to keep track of the reduction in OCV as the cell discharged. The inset illustrates the capability of the optimizer to capture the dynamics of the system. The remarkable agreement with which such a simple equivalent circuit was able to simulate cell behavior made this approach especially suitable to develop control algorithms and system level models.

A. Look-up Tables

Figures 8-11 show the result of the parameter estimation procedure. These values constitute the look-up tables for the non-isothermal model. Figure 8 shows how the e.m.f., represented here by the voltage source E_m , strongly depends upon the SOC, while being largely independent of temperature. Figures 9-11 show the variation of R_0 , R_1 and C_1 with temperature and state of charge.

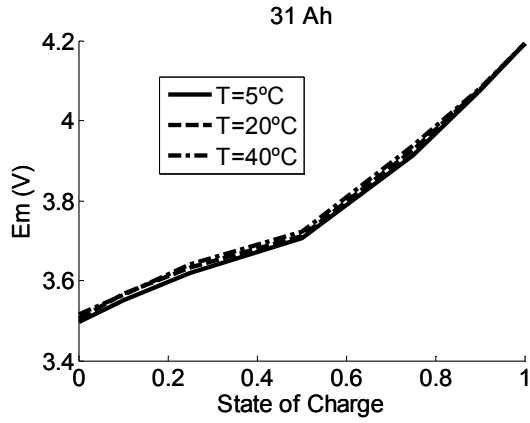


Figure 8. Electro-motive force (E_m) as a function of T and SOC. Temperature dependence is minimal compared to SOC dependence.

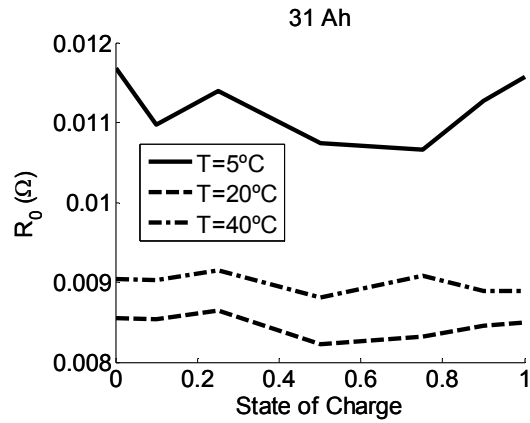


Figure 9. Ohmic internal resistance R_0 shows much stronger dependence on temperature than on SOC, suggesting ion movement across the separator as responsible for this component of energy losses. The resistance decreases for high temperatures.

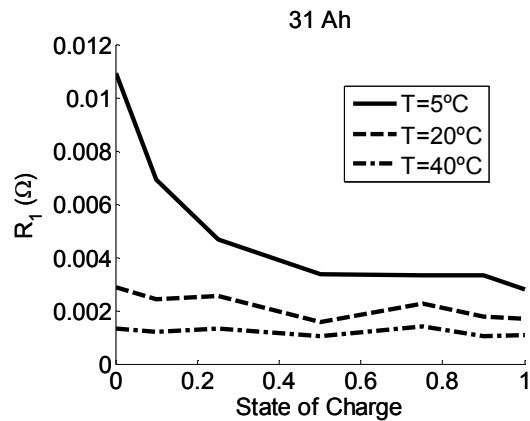


Figure 10. R_1 , the resistive component of the RC element, inversely depends on temperature, but only shows SOC dependence at 5°C.

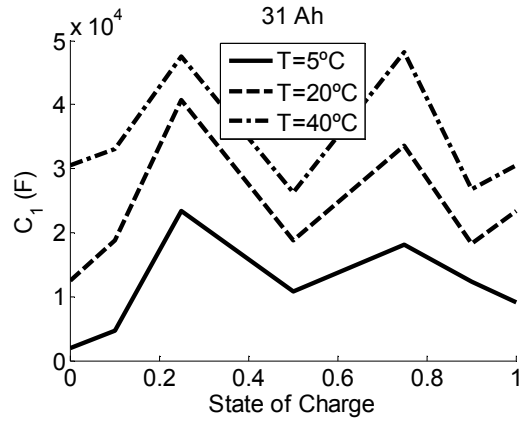


Figure 11. The capacitive component of the RC element seems to depend on temperature, but it also shows a jagged shape with SOC. The reason for this behavior is not clear at this moment.

B. Validation

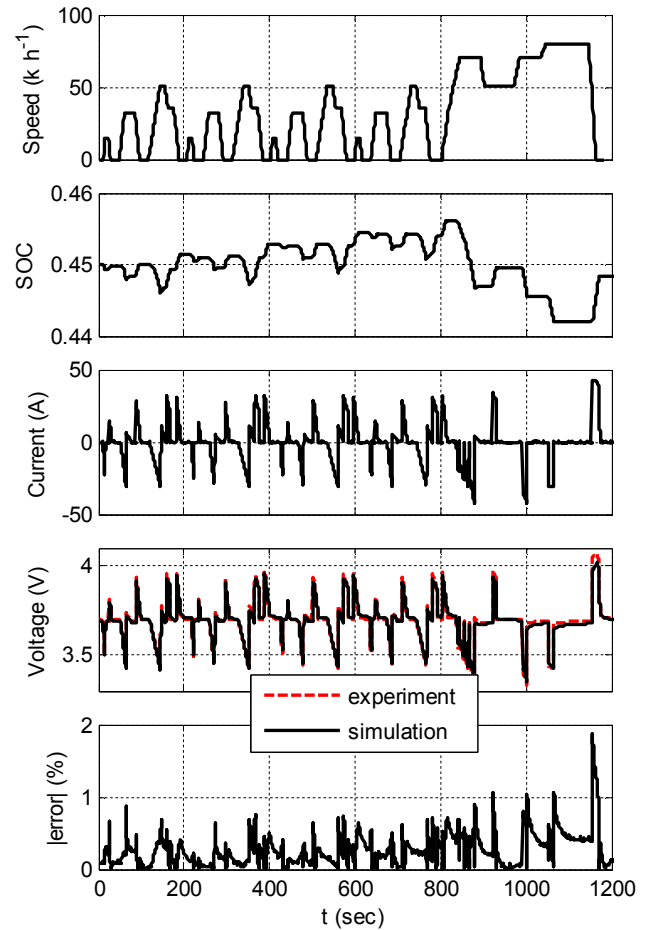


Figure 12. Validation. Top to bottom: Speed: vehicle speed during New European Drive Cycle. SOC: simulated state-of-charge. Current: electrical current corresponding to the New European Driving Cycle. Voltage: Experimental (dashed red) and simulated (solid black) potential (V) evolution as a result of the input. |error|: voltage discrepancy between model and experiment (%).

Validation of the proposed approach required comparison with an independent set of experimental data. The New European Driving Cycle, featuring the current profile shown in Figure 12 was used to this effect. The voltage plot of this figure shows the simulation result and the experimental measurement for the voltage delivered by the cell. The error graph shows the percentage difference between these voltages, which remains below 2%. Figure 13 shows a close-up view of the voltage difference enduring the latter part of the 20-minute cycle.

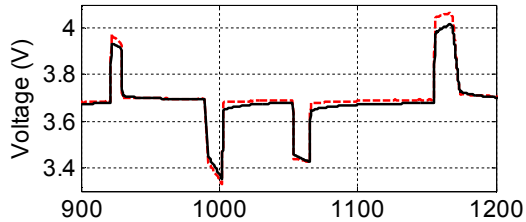


Figure 13. Voltage discrepancy at end of New European Drive Cycle.

The experimental conditions for this measurement were: $T = 20^{\circ}\text{C}$, and initial SOC = 45%. Figure 12 also shows the speed profile and online state of charge estimation computed solely by coulomb counting. During the rest period after the cycle, the SOC could be corrected using the SOC-OCV correlation from the lookup tables in this model. Techniques such as the extended Kalman filter approach [4-6] could enhance the SOC correction.

C. Simulation

The isothermally-validated model can now be expanded to consider thermal effects. Additions to the model that allow this expansion include:

- Convective heat exchange between the cell and the environment
- Calculation of heat losses due to internal resistances
- Thermal mass of cell assembly
- Two-dimensional look-up tables for equivalent circuit elements.

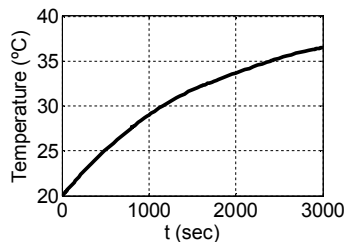


Figure 14. Temperature increase for a constant current discharge of 3000 sec at 31 A.

An interesting example of application for this model is the calculation of the temperature build-up

during a constant current discharge. Figure 14 shows the temperature evolution for the following constant current discharge situation:

- Current discharge: 31 A
- Ambient temperature: 20°C

The resulting temperature increase in this situation was approximately 16°C .

The thermal parameters utilized in this simulation were:

- Convective heat exchange coefficient between the cell and the environment $R_T = 5 \text{ W m}^{-2} \text{ K}^{-1}$
- Cell heat capacity $C_T = 2.04 \times 10^6 \text{ J m}^{-3} \text{ K}^{-1}$
- Cell dimensions: $0.0084 \times 0.215 \times 0.22 \text{ m}^3$

The convective heat transfer coefficient must be set based on the experimental conditions or design requirements.

For integration into system level models, the ambient temperature can be easily set as an input variable that accepts a temperature reading from other part of the model, for example a thermodynamic model of a hybrid vehicle.

VI. CONCLUSIONS

This work expands upon the general structure of the equivalent circuit cell model presented in prior literature [1-2, 10-11] by including cell thermal dynamics. The paper illustrates a practical method for evaluating the equivalent circuit parameters using pulse discharge experimental data to create lookup tables with cell temperature and SOC as independent variables.

For the $\text{LiNi}_x\text{Mn}_y\text{Co}_z\text{O}_2$ (NMC) cell chemistry under study, an equivalent circuit with a voltage source, a series resistor, and a single RC element was adequate to capture the dynamics of the system. The techniques used for evaluating the parameters could also be used for an equivalent circuit model of higher complexity to better fit experimental data.

The model was validated using a single 20-minute New European Drive Cycle, which showed cell voltage accuracy within 2%. The model accounts for the inner heat generated in the cell and the corresponding thermal build-up; and predicted the cell voltage and SOC for an arbitrary current profile. The procedure also illustrates a way in which Simscape™ may be utilized as a numerical tool for modeling electrochemical systems using equivalent circuits, in combination with the parameter estimation functionalities of Simulink Design Optimization™.

A simple single-cell thermal model was developed in this paper. However, cells are generally combined into cell packs, whose thermal parameters are different from those of single isolated cells. This case has not been considered in this article, but shall be the subject of a future contribution. Future work shall also investigate

the dependence of the equivalent circuit model parameters on current magnitude.

VII. REFERENCES

- [1] M. Ceraolo, G. Lutzemberger, T. Huria, "Experimentally-Determined Models for High-Power Lithium Batteries", *Advanced Battery Technology 2011*, SAE, April 2011. ISBN: 978-0-7680-4749-3. doi: 10.4271/2011-01-1365
- [2] Min Chen; G.A. Rincon-Mora, "Accurate electrical battery model capable of predicting runtime and I-V performance," *Energy Conversion, IEEE Transactions on*, vol.21, no.2, pp. 504- 511, June 2006. doi: 10.1109/TEC.2006.874229
- [3] M.A. Roscher, J. Assfalg, O.S. Bohlen, "Detection of Utilizable Capacity Deterioration in Battery Systems," *Vehicular Technology, IEEE Transactions on*, vol.60, no.1, pp.98-103, Jan. 2011. doi: 10.1109/TVT.2010.2090370
- [4] G. L. Plett, "Extended Kalman filtering for battery management systems of LiPB-based HEV battery packs. Part 1. Background," *Journal of Power Sources*, vol. 134, pp. 252-261, 2004.
- [5] G. L. Plett, "Extended Kalman filtering for battery management systems of LiPB-based HEV battery packs. Part 2. Modeling and identification," *Journal of Power Sources*, vol. 134, pp. 262-276, 2004.
- [6] G. L. Plett, "Extended Kalman filtering for battery management systems of LiPB-based HEV battery packs. Part 3. State and parameter estimation," *Journal of Power Sources*, vol. 134, pp. 277-292, 2004.
- [7] Marc Doyle, Thomas F. Fuller, and John Newman, "Modeling of Galvanostatic Charge and Discharge of the Lithium/Polymer/Insertion Cell", *J. Electrochem. Soc.* 140, 1526 (1993), doi:10.1149/1.2221597
- [8] Thomas F. Fuller, Marc Doyle, and John Newman, "Simulation and Optimization of the Dual Lithium Ion Insertion Cell", *J. Electrochem. Soc.* 141, 1 (1994), doi:10.1149/1.2054684
- [9] Tsutomu Ohzuku, Yoshinari Makimura, "Layered Lithium Insertion Material of LiCo1/3Ni1/3Mn1/3O2 for Lithium-Ion Batteries", *Chemistry Letters*, Vol. 30 (2001) , No. 7 p.642. doi: 10.1246/cl.2001.642.1246/cl.2001.642
- [10] M. Ceraolo: "New Dynamical Models of Lead-Acid Batteries", *IEEE Transactions on Power Systems*, November 2000, Vol. 15, N. 4, pp. 1184-1190.
- [11] S. Barsali, M. Ceraolo: "Dynamical models of lead-acid batteries: implementation issues", *IEEE Transactions on Energy Conversion*, Vol. 17, N. 1, Mar 2002, Pages 16-23.
- [12] S. Piller, M. Perrin, A. Jossen, "Methods for state-of-charge determination and their applications", *J. Power Sources* 96(2001) 113-120.
- [13] 31Ah Kokam SLPB 78216216H cell, http://www.kokam.com/new/kokam_en/sub01/sub01_01.html
- [14] Robyn A. Jackey, "A Simple, Effective Lead-Acid Battery Modeling Process for Electrical System Component Selection," SAE Paper 2007-01-0778, SAE International, Warrendale, PA, 2007.
- [15] Robyn A. Jackey, G. L. Plett, M. J. Klein "Parameterization of a Battery Simulation Model Using Numerical Optimization Methods," SAE Paper 2009-01-1381, SAE International, Warrendale, PA, 2009.



Tarun Huria was born in 1973 in India. He received his M.S. degree in information technology from Punjab Technical University, Jalandhar, India in 2004, and since 2009 has been working towards his Ph.D. degree in land vehicles and transport systems from the University of Pisa, Italy.

He worked for the Indian Railways from 1995 to 2009. His research interests include modelling and control of hybrid electric vehicles and energy storage, especially for heavy road and rail vehicles.



Massimo Ceraolo was born in 1960. He received his Master's degree (with honors) in electrical engineering from the University of Pisa, Italy in 1985.

He is currently a Full Professor of electric power systems and on-board electric systems at the University of Pisa, Italy. He also teaches naval electric systems at the Italian Naval Academy, Livorno, Italy. His research interests include electrochemical systems and electric, hybrid electric and fuel cell vehicles.

Javier Gazzarri received his bachelor's degree in mechanical engineering from the Universidad de Buenos Aires, Argentina in 1998. He completed his MASc and PhD degrees in mechanical engineering from the University of British Columbia, Vancouver, Canada in 2003 and 2008 respectively.



He is currently a Senior Application Engineer at MathWorks, Detroit in the area of Physical Modeling. His expertise includes numerical modeling and simulation, finite element analysis, battery and fuel cell technology, transport phenomena, degradation and diagnosis of electrochemical systems, optimization, impedance spectroscopy, and inverse analysis. Prior to joining MathWorks, he worked at the National Research Council of Canada, Institute for Fuel Cell Innovation, as a research scientist in the area of fuel cell modeling, and at Tenaris-Siderca as a research engineer in the area of materials characterization.



Robyn A. Jackey received his B.S. and M.S. degrees in electrical engineering from Clarkson University, USA in 2001 and 2002 respectively.

He is a Senior Technical Consultant at MathWorks, Novi, MI. He specializes in modeling, simulation, and automatic code generation, primarily for clients in the automotive and aerospace industries. His recent work includes modeling and simulation of chemical batteries, software development, and implementation of Model-Based Design simulation tools in large organizations.